

Caralumane Superacids of Lewis and Brønsted Character

Published as part of *The Journal of Physical Chemistry virtual special issue "Alexander Boldyrev Festschrift"*.

Jakub Brzeski, Piotr Skurski, and Jack Simons*



Cite This: *J. Phys. Chem. A* 2021, 125, 999–1011



Read Online

ACCESS |



Metrics & More

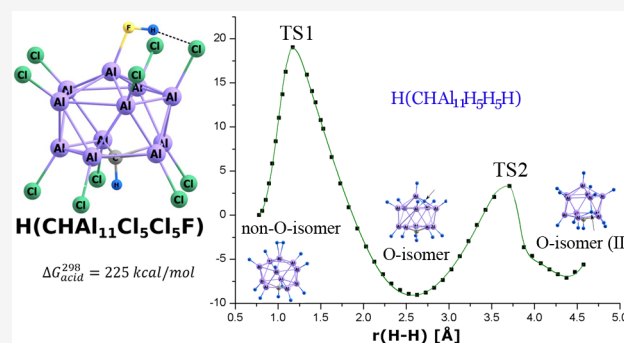


Article Recommendations



Supporting Information

ABSTRACT: Carborane Brønsted superacids have proven to be useful reagents in a variety of organic and inorganic synthetic processes. In this work, analogs in which the icosahedral CB_{11} carborane core is replaced by a CA_{11} core are studied using ab initio electronic structure tools. Each so-called caralumane Brønsted acid is formed by adding HF, HCl, or HH to a corresponding caralumane Lewis acid possessing a vacant Al-centered orbital that acts to accept an electron pair from the HF, HCl, or HH. The Lewis acid strengths of the species involved, as measured by their F^- ion affinities, are all found to exceed the threshold for labeling them Lewis superacids. Also, the deprotonation Gibbs free energies of the Brønsted acids are found to be small enough for them to be Brønsted superacids. When HF or HCl is bound to a caralumane Lewis acid to form the Brønsted acid, the HF or HCl is bound datively to a single Al atom, and hydrogen bonds can be formed between this molecule's H atom and nearby F or Cl atoms attached to other Al atoms. In contrast, when HH is bound to the Lewis acid to form the Brønsted acid, two novel low-energy structures arise, both of which are Brønsted superacids. One has an essentially intact HH molecule attached to a single Al atom in a η^2 fashion. In the other, the HH molecule is heterolytically cleaved to generate a hydride ion that attaches to a single Al atom and a proton that binds in a multicenter manner to other Al atoms. The structures and relative energies of a multitude of such caralumane Lewis and Brønsted superacids are provided and discussed.



1. INTRODUCTION

In this work, we focus on a family of compounds analogous to the widely studied carboranes each of which consists of a cage containing one CH unit and 11 Al atoms 10 of which are bonded to an H, F, or Cl atom. These molecules are shown to be Lewis superacids that form Brønsted superacids when an HH, HF, or HCl molecule (acting as a Lewis base) is bonded to them. We call these caralumane Lewis and Brønsted superacids.

1.1. What Are Superacids? To be categorized as a superacid, certain criteria must be met. A Lewis acid's strength is often measured in terms of its fluoride ion affinity (FIA) in the gas phase.¹ For example, the FIAs of BF_3 and PF_5 (strong Lewis acids) are 81 and 94 kcal/mol, respectively.² Lewis superacids are usually classified as compounds having FIA values exceeding that of SbF_5 (ca. 120 kcal/mol).³ The acidity of Brønsted acids is commonly expressed as the value of the gas-phase Gibbs free energy of deprotonation at $T = 298.15$ K (denoted ΔG_a^{298}),^{4,5} and the ΔG_a^{298} of 303 kcal/mol for anhydrous H_2SO_4 ⁶ is usually considered the threshold separating regular Brønsted acids from superacids. In this work, we demonstrate that our Brønsted acids have ΔG_a^{298} values below 303 kcal/mol and the corresponding Lewis acids have FIA values in excess of 120 kcal/mol.

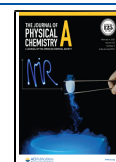
While discussing the Lewis and Brønsted superacids that we focus on in this work, it is important to recognize the connection between the Lewis and Brønsted aspects of these species. To illustrate, one of the Lewis acids we treat here has its structure shown in Figure 1 along with its boron-containing analog. The $CHAl_{11}F_5F_5$ molecule has one Al atom whose vacant 3p lowest unoccupied molecular orbital (LUMO) serves as the electron-pair accepting site when it acts as a Lewis acid to bind, for example, an HF or HCl molecule acting as a Lewis base to then form the Brønsted acid $H(CHAl_{11}F_5F_5)$ or $H(CHAl_{11}F_5F_5Cl)$. This same LUMO is the site that a fluoride ion is bound when discussing the FIA, which we mentioned earlier is used as a measure of acid strength for Lewis acids.

Clearly there are differences between the B- and Al-containing species. The latter is larger, reflecting the Al and B atomic size difference, the LUMO orbital is more localized (on the B atom) in the former, and the LUMO is more

Received: December 9, 2020

Revised: January 13, 2021

Published: January 22, 2021



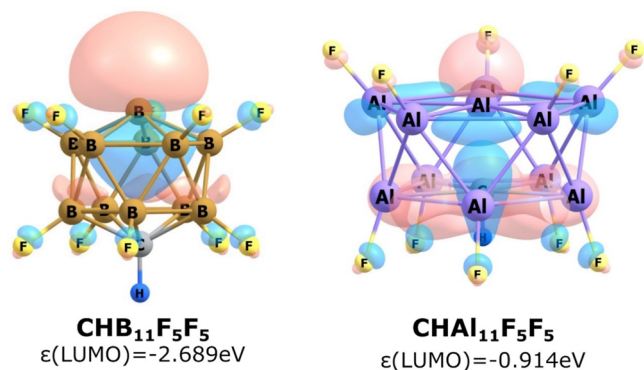


Figure 1. Equilibrium structures of one boron-based and one aluminum-based Lewis acid unit showing the LUMO that acts as the electron pair acceptor in the Lewis acid sense. Also shown are the Koopmans theorem (KT) orbital energies of these vacant orbitals.

delocalized in the latter. However, as will be demonstrated throughout this manuscript, there are many similarities in the chemical properties of the B- and Al-containing species.

1.2. Chemical Applications of Superacids. Anions such as those formed by deprotonation of the superacids treated here are often referred to as *weakly coordinating anions*, WCAs,^{7,8} but they are not *superhalogen anions*⁹ because their electron binding energies do not exceed those of halide ions (ca. 3.5 eV). The existence of superhalogen anions was originally postulated by Gutsev and Boldyrev in 1981, and this was followed by many studies concerning various compounds of that kind.^{9–17} The Al-containing anion formed by adding an electron to the species shown in Figure 1 would not be termed a superhalogen anion since its electron binding energy, approximated through the Koopmans' theorem LUMO orbital energy, does not exceed 3.5 eV.

Applications of WCAs include being counterions in catalysts involving highly reactive metal cations^{18–20} and acting as counterions to Li^+ cations lithium-ion batteries.²¹ The search for very stable anions capable of forming highly conductive salts with Li^+ is thought to be a promising way to design more effective batteries of that type.²² Although some of the simplest chemically inert anions (e.g., BF_4^- and PF_6^-)²³ are commonly used as the negatively charged components of many ionic liquids,^{24–26} the breakthrough in the area of designing new WCAs came with the development of the so-called BARF (tetrakis(3,5-bis(trifluoromethyl)phenyl)borate)²⁷ characterized by even weaker coordinating properties than the tetrafluoroborate or hexafluorophosphate anions. In particular, BARF has been used to form salts involving cations that have not been isolated earlier, such as diethyl ether oxonium ion²⁷ or the highly unstable $[\text{PdCl}(\text{TeMe}_2)_3]^+$ cation.²⁸ An important family of chemically inert anions related to those studied here are based on the $(\text{CHB}_{11}\text{H}_3\text{H}_5\text{H})^-$ carborane ion (often written as $\text{CHB}_{11}\text{H}_{11}^-$) and its derivatives^{29,30} which were shown to stabilize even as fragile cations as C_{60}^+ , AlEt_2^+ , and C_6H_7^+ .^{31–33}

A group of Brønsted superacids that has been attracting attention for last two decades is the family of carborane acids whose acid strength is related to the large stability of the icosahedral CB_{11} “carborane core”. The synthesis of the $(\text{CHB}_{11}\text{H}_3\text{H}_5\text{H})^-$ anion by Knoth in 1967³⁴ paved the way for the Reed group to synthesize and investigate various carborane acids and their corresponding conjugate bases. In addition to many important findings reported by Reed and co-workers

concerning this subject, they managed to isolate the $\text{H}(\text{CHB}_{11}\text{H}_3\text{Cl}_5\text{Cl})$ superacid³⁵ and to determine the structure of the $\text{H}(\text{CHB}_{11}\text{Cl}_5\text{Cl}_5\text{Cl})$ superacid.³⁶ Also, they showed evidence for C–H...Cl hydrogen bonding in the $(\text{C}(\text{CH}_3)_3)^+ / (\text{CHB}_{11}\text{Cl}_5\text{Cl}_5\text{Cl})^-$ salt³⁷ and described the protonation of butane by $\text{H}(\text{CHB}_{11}\text{F}_5\text{F}_5)$ acid at room temperature.³⁸ Recently, the Reed group reported results concerning protonation of highly inert species, such as carbon dioxide, using carborane superacids.³⁹ Many other groups have also contributed to the field by investigating various carborane acids and their conjugate bases.^{40–46} In addition, the Skurski group has recently shown the large mobility of the acidic proton in certain carborane acids and a significant increase of their acid strength upon dimerization.⁴⁷

1.3. Lewis and Brønsted Superacids Treated Here.

Keeping in mind the usefulness of carborane acids, we decided to investigate the possible existence and stability of their analogues having all boron atoms replaced with aluminum atoms. To the best of our knowledge, such compounds have never been described in the literature thus far. As this effort is our first aimed at characterizing this new class of superacids, we restrict our attention to characterizing the species isolated from any solvation environment although we realize that the corresponding carborane-based superacids have been utilized in many synthetic reactions taking place in a wide variety of solvents and with other reagents present.

Before proceeding to discuss our methods and results, it is important to make clear the notation we use to describe the mixed Lewis–Brønsted acids discussed here.

1.3.a. Lewis Acid Nomenclature. As can be seen in Figures 1 and 2 and as will be clear in subsequent figures showing

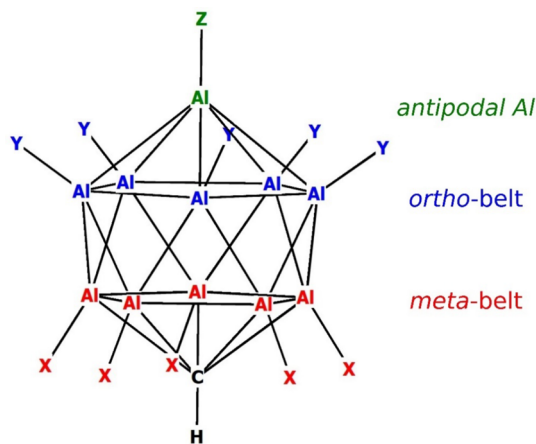


Figure 2. Scheme illustrating the $(\text{CHAl}_{11}\text{X}_5\text{Y}_5\text{Z})$ notation used to label various positions on the CA_{11} cage.

molecular structures, each neutral Lewis acid molecule has one C–H unit (shown at the bottom) bonded within a cage structure containing 11 B or Al atoms. In the neutral Lewis acid, ten of the B or Al atoms have an H, F, or Cl atom attached while the 11th (antipodal) B or Al atom has a vacant 2p or 3p orbital as shown in Figure 1. Such a neutral Lewis acid is written, for example, as $\text{CHAl}_{11}\text{H}_3\text{H}_5$, $\text{CHB}_{11}\text{F}_5\text{F}_5$, or $\text{CHAl}_{11}\text{Cl}_5\text{Cl}_5$. When there exists a mixture of H, F, and Cl atoms bonded to the five ortho-belt and five meta-belt Al or B atoms, we use, for example, $\text{CHAl}_{11}\text{F}_5\text{Cl}_5$ or $\text{CHB}_{11}\text{Cl}_5\text{H}_5$ to label the Lewis acids, with the atoms closest to the Al or B residing in the meta-positions and those to the right residing in

the ortho-positions. We should also mention that we only considered in this work structures for the Lewis acids that preserve C_{5v} symmetry.

1.3.b. Brønsted Acid Nomenclature. When an HF, HCl, or HH molecule attaches to the vacant 2p or 3p site on the top B or Al atom, a Brønsted acid is formed from the original Lewis acid. For the first two Lewis acid cases mentioned above, $\text{CHAl}_{11}\text{H}_5\text{H}_5$ and $\text{CHB}_{11}\text{F}_5\text{F}_5$, the corresponding Brønsted acids are denoted $\text{H}(\text{CHAl}_{11}\text{H}_5\text{H}_5\text{F})$ or $\text{H}(\text{CHB}_{11}\text{F}_5\text{F}_5\text{F})$, when HF is added, $\text{H}(\text{CHAl}_{11}\text{H}_5\text{H}_5\text{Cl})$ or $\text{H}(\text{CHB}_{11}\text{F}_5\text{F}_5\text{Cl})$, when HCl is added, and $\text{H}(\text{CHAl}_{11}\text{H}_5\text{H}_5\text{H})$ or $\text{H}(\text{CHB}_{11}\text{F}_5\text{F}_5\text{H})$, when HH is added. More generally, when HZ is added to $\text{CHAl}_{11}\text{X}_3\text{Y}_5$, $\text{H}(\text{CHAl}_{11}\text{X}_3\text{Y}_5\text{Z})$ is formed which has the X atoms in the meta-positions near the carbon, the Y atoms in the ortho-positions near the top (i.e., antipodal) Al atom and the Z atom bonded to this Al atom.

As will be shown later when the structures of these Brønsted acids are displayed, when HF or HCl binds to the Lewis acid, the halogen donates a lone electron pair into the vacant B or Al p orbital and the FH or ClH bond orients itself to form a hydrogen bond to a neighboring ortho-belt atom if the ortho belt is occupied by halogen atoms. If the ortho belt contains only H atoms, such hydrogen bonds are not present.

When HH binds to the Lewis acid, something very different happens. For both the B-containing and Al-containing species, two low-energy local-minimum structures are formed, both of which we consider in this work. One consists of an essentially intact HH molecule sitting directly above the antipodal B or Al atom and involves an unusual donation of electron pair density from the HH molecule's $1\sigma^2$ density. To the best of our knowledge, these structures have not been identified in earlier studies of the B-containing molecules. The other structure consists of an HH molecule that has been heterolytically cleaved and has one of its H atoms attached to the antipodal B or Al atom as a hydride ion while the other H atom is located between the antipodal atom and two ortho-belt atoms or between the ortho- and meta-belt atoms as a proton. The latter structures have been seen in earlier studies of the B-containing species, for example by the Ortiz group.⁴³ In Figure 3, we show the antipodal-bonded and the ortho-belt localized structures for $\text{H}(\text{CHB}_{11}\text{H}_5\text{H}_5\text{H})$ to illustrate the differences in bonding.

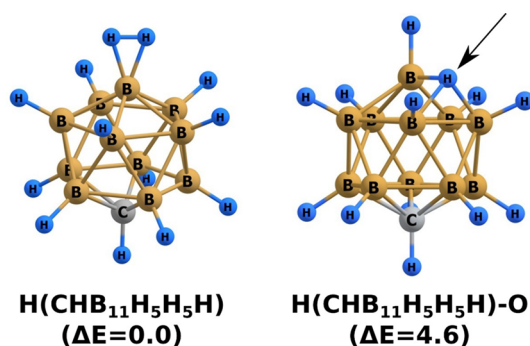


Figure 3. Two local-minimum structures arising when HH is added to $(\text{CHB}_{11}\text{H}_{10})$. The structure with the HH molecule tethered to the antipodal B atom is shown on the left whereas the structure containing cleaved HH (labeled with the O symbol in the text) is shown on the right. In the O structure one H atom is bound to the antipodal B atom while the other H atom (indicated by an arrow) is located between the antipodal B and two ortho-belt B atoms. The relative energies (ΔE) of these isomers are given in kcal/mol.

Throughout this work, the structures in which the HH molecule has been cleaved will be labeled with the O symbol to differentiate them from the structures with the HH molecule sitting on top.

Later in this manuscript, we will see that for some of the B- and Al-containing compounds treated here, the structure labeled O is lower in energy than the alternative structure, while for other compounds, the structure labeled O is higher in energy. Also later, we will have more to say about this issue where we illustrate the intrinsic reaction paths and corresponding energy barriers connecting these two alternative structures. Because the two structures are close in energy for most of the cases studied here, we believe it is important to consider both of them throughout this study.

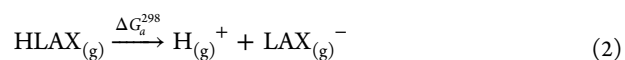
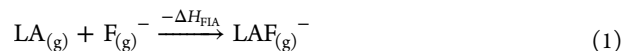
1.3.c. The Fluoride Ion Adduct Nomenclature. When a F^- ion is attached to the antipodal B or Al atom's 2p or 3p orbital of a Lewis acid a fluoride-ion adduct is formed. For the first two Lewis acids illustrated in Figure 1, $\text{CHAl}_{11}\text{H}_5\text{H}_5$ and $\text{CHB}_{11}\text{F}_5\text{F}_5$, the fluoride ion adducts are expressed as $(\text{CHAl}_{11}\text{H}_5\text{H}_5\text{F})^-$ and $(\text{CHB}_{11}\text{F}_5\text{F}_5\text{F})^-$ with the last F atom representing the F^- ion bonded to the top Al or B atom. In like fashion, we use $(\text{CHAl}_{11}\text{H}_5\text{H}_5\text{H})^-$ and $(\text{CHAl}_{11}\text{H}_5\text{H}_5\text{Cl})^-$ to describe the addition of an H^- or Cl^- ion to $\text{CHAl}_{11}\text{H}_5\text{H}_5$.

In the following sections, we first describe the methods we used to obtain our results and then we move on to (i) characterize the Lewis and Brønsted acid characters and strengths of the superacids studied here, (ii) describe the bonding and geometries arising in the Lewis and Brønsted acids, and (iii) emphasize connections between the Lewis and Brønsted characters of these species. In the final section, we offer conclusions and summarize our findings.

2. METHODS

The stationary-point structures of all systems investigated were obtained by applying the second-order Møller–Plesset perturbation method (MP2)^{48–50} with valence basis sets of double- ζ quality: aug-cc-pVDZ for H, C, F, and Cl^{51} and aug-cc-pV(D+d)Z⁵² for B and Al. The harmonic vibrational frequencies characterizing the stationary points were evaluated at the same MP2/aug-cc-pVDZ/aug-cc-pV(D+d)Z theory level to ensure that all the obtained structures correspond to true minima or first-order saddle points on the potential energy surface.

Both the enthalpies (ΔH) for fluoride ion addition to Lewis acids (FIA) and Gibbs free energies of the deprotonation of the Brønsted acids reactions (ΔG_a^{298}) were evaluated using the electronic energies, zero-point energy corrections, and thermal corrections (at $T = 298.15$ K). Moreover, for the calculations of Gibbs free energies, entropy contributions were included. All thermochemical calculations were performed at the MP2 level using the basis sets discussed earlier. In each case, the Gibbs free energy of the proton was also accounted for. The fluoride ion affinity (FIA) of Lewis acids and gas-phase acidities of Brønsted acids are defined according to eqs (1) and (2):



where LA represents the Lewis acid and X stands for H, F, or Cl.

For reasons of consistency, we used enthalpies determined at the MP2/aug-cc-pVDZ/aug-cc-pV(D+d)Z theory level for the electron affinities (EA) of H, F, and Cl, ionization potential (IP) of H, and dissociation energies (D_e) of HF, HCl, and HH, rather than precise literature values while discussing the thermodynamic cycle relating to the Lewis and Brønsted characters of the $H(\text{CHAl}_{11}\text{X}_5\text{Y}_5\text{Z})$ and $H(\text{CHB}_{11}\text{X}_5\text{Y}_5\text{Z})$ species.

Although the emphasis of this work is on Al-containing species, we include results for several B-containing systems, some of which have been studied earlier and some of which have not, to show similarities and differences between the two classes of molecules. All calculations were carried out using the GAUSSIAN16 (Rev.B.01) package.⁵³

3. RESULTS

The Cartesian coordinates corresponding to the equilibrium structures of the Brønsted superacids $H(\text{CHX}_{11}\text{Y}_{10}\text{Z})$ (where $X = \text{B}, \text{Al}$; $Y, Z = \text{H}, \text{F}, \text{Cl}$) and $H(\text{CHAl}_{11}\text{X}_5\text{Y}_5\text{Z})$ (where $X, Y, Z = \text{H}, \text{F}, \text{Cl}$), their conjugate bases (i.e., the anions formed by deprotonation thereof), and their corresponding Lewis acids (i.e., the systems formed by detaching the H–Z unit, where Z stands for H, F, or Cl) are provided in the Supporting Information (Table S1).

3.1. The Lewis and Brønsted Nature of Carborane and Caralumane Acids. To illustrate the Lewis acid aspect of the species considered here, we showed in Figure 1 one boron-based and one aluminum-based Lewis acid, $\text{CHB}_{11}\text{F}_5\text{F}_5$ and $\text{CHAl}_{11}\text{F}_5\text{F}_5$. Each of these neutral molecules has one B or Al atom (at the top of Figure 1) with a vacant orbital (of largely 2p or 3p character, respectively) that acts as the electron-pair acceptor in its Lewis acid behavior. The Koopmans theorem orbital energies of these vacant orbitals (-2.689 and -0.914 eV for the boron and aluminum systems, respectively) are quite substantial but not large enough to call the anions formed by adding an electron superhalogens.

From each of the several Lewis acid units considered here, a Brønsted acid is formed by binding one HF, HCl, or HH molecule to the Lewis acid with the HF, HCl, or HH acting as an electron-pair donor Lewis base. In Figure 4, we show two examples of aluminum-based systems with an HF or HCl molecule attached.

Notice that the Lewis base's halogen atom is bonded to the top Al atom and that its H atom forms a hydrogen bond to a nearby F atom. Later we will show geometries for all of the Lewis acid and Brønsted Al-based acids studied here, where similar geometrical features will appear but where somewhat

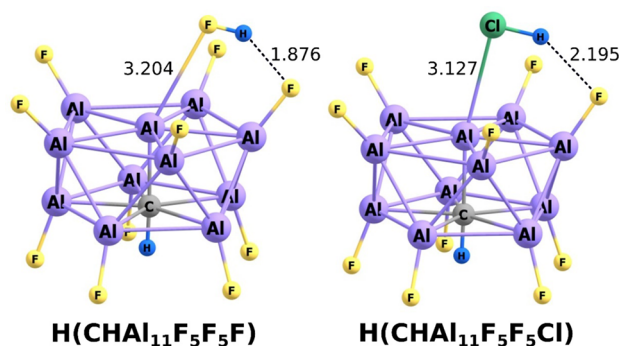
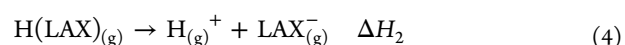
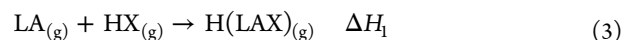


Figure 4. Equilibrium structures of two representative Brønsted caralumane superacids. Selected bond lengths are given in Å.

unusual structures arise when HH serves as the Lewis base as mentioned earlier when discussing Figure 3.

3.2. Acid Strengths and Geometries of the Acids.

When acting as Brønsted acids, the species just discussed dissociate to produce H^+ ions and closed-shell anions such as $(\text{CHAl}_{11}\text{F}_5\text{F}_5)^-$ and $(\text{CHAl}_{11}\text{F}_5\text{F}_5\text{Cl})^-$ for the two examples introduced above. Denoting the Lewis acid building block for each species as LA and using HX to label HF, HCl, or HH, the following reactions' thermochemistry are useful to consider:



The first reaction involves LA acting as a Lewis acid (and ΔH_1 is expected to be negative), while the second involves H(LAX) acting as a Brønsted acid with (positive) ΔH_2 being the gas-phase proton affinity (PA) of the $(\text{LAX})^-$ anion.

It is possible to connect the Lewis and Brønsted strength values using the closed thermodynamic cycle shown in Figure 5.

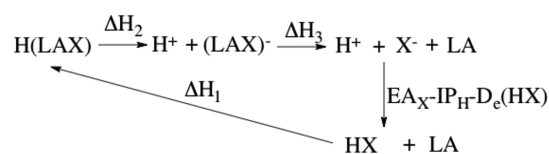


Figure 5. Closed thermodynamic cycle relating the Lewis and Brønsted characters of the $H(\text{CHAl}_{11}\text{X}_5\text{Y}_5\text{Z})$ and $H(\text{CHB}_{11}\text{X}_5\text{Y}_5\text{Z})$ species.

Specifically, the sum of the Lewis and Brønsted ΔH values ($\Delta H_1 + \Delta H_2$) plus the X^- ion affinity of LA (ΔH_3) should add up to the sum of the ionization potential of H plus the bond dissociation energy D_e of the HX molecule minus the electron affinity of X. To be a bit more precise, because we use enthalpies $\Delta H_{1,2,3}$ for three of these values, we have also used enthalpies for the EA, IP, and D_e values in making use of this cycle (see later in Tables 3 and 4).

3.2.1. Lewis Acid Strengths. In Table 1, we list the fluoride ion affinities of each of the Lewis acids, and in Table 2 we

Table 1. Fluoride Ion Affinities of the Lewis Superacids

Lewis superacid	FIA [kcal/mol]
$\text{CHAl}_{11}\text{H}_5\text{H}_5$	134.7
$\text{CHB}_{11}\text{H}_5\text{H}_5$	132.3
$\text{CHAl}_{11}\text{F}_5\text{F}_5$	132.6
$\text{CHB}_{11}\text{F}_5\text{F}_5$	178.7
$\text{CHAl}_{11}\text{Cl}_5\text{Cl}_5$	143.8
$\text{CHB}_{11}\text{Cl}_5\text{Cl}_5$	178.7
$\text{CHAl}_{11}\text{F}_5\text{H}_5$	133.9
$\text{CHAl}_{11}\text{H}_5\text{F}_5$	144.8
$\text{CHAl}_{11}\text{Cl}_5\text{H}_5$	140.8
$\text{CHAl}_{11}\text{H}_5\text{Cl}_5$	148.3
$\text{CHAl}_{11}\text{F}_5\text{Cl}_5$	137.2
$\text{CHAl}_{11}\text{Cl}_5\text{F}_5$	139.7

show the Gibbs free energy changes ΔG_a^{298} for deprotonation of each of the Brønsted acids. Finally, in Tables 3 and 4, we show the Brønsted ΔH_2 deprotonation values, the ΔH_1 values related to forming the Brønsted acid from the corresponding

Table 2. Gibbs Free Energies for Deprotonating the Carborane and Caralumane Brønsted Superacids

Lewis–Brønsted superacid	ΔG_a^{298} [kcal/mol]
H(CHAl ₁₁ H ₅ H ₅ H)	265.8
H(CHAl ₁₁ H ₅ H ₅ H)-O	273.2
H(CHB ₁₁ H ₅ H ₅ H)	261.6
H(CHB ₁₁ H ₅ H ₅ H)-O	256.0
H(CHAl ₁₁ H ₅ H ₅ F)	239.9
H(CHAl ₁₁ H ₅ H ₅ Cl)	240.4
H(CHAl ₁₁ F ₅ F ₅ H)	265.9
H(CHAl ₁₁ F ₅ F ₅ H)-O	251.4
H(CHAl ₁₁ F ₅ F ₅ F)	238.0
H(CHB ₁₁ F ₅ F ₅ F)	218.0
H(CHAl ₁₁ F ₅ F ₅ Cl)	238.5
H(CHAl ₁₁ Cl ₅ Cl ₅ F)	225.0
H(CHAl ₁₁ Cl ₅ Cl ₅ H)	252.3
H(CHAl ₁₁ Cl ₅ Cl ₅ H)-O	248.2
H(CHAl ₁₁ Cl ₅ Cl ₅ Cl)	226.9
H(CHB ₁₁ Cl ₅ Cl ₅ Cl)	228.6
H(CHAl ₁₁ H ₅ F ₅ H)	256.1
H(CHAl ₁₁ H ₅ F ₅ H)-O	263.8
H(CHAl ₁₁ H ₅ F ₅ F)	235.6
H(CHAl ₁₁ H ₅ F ₅ Cl)	235.0
H(CHAl ₁₁ F ₅ H ₅ H)	264.4
H(CHAl ₁₁ F ₅ H ₅ H)-O	261.3
H(CHAl ₁₁ F ₅ H ₅ F)	231.9
H(CHAl ₁₁ F ₅ H ₅ Cl)	235.5
H(CHAl ₁₁ H ₅ Cl ₅ H)	253.3
H(CHAl ₁₁ H ₅ Cl ₅ H)-O	259.7
H(CHAl ₁₁ H ₅ Cl ₅ F)	233.5
H(CHAl ₁₁ H ₅ Cl ₅ Cl)	234.2
H(CHAl ₁₁ Cl ₅ H ₅ H)	253.7
H(CHAl ₁₁ Cl ₅ H ₅ H)-O	259.4
H(CHAl ₁₁ Cl ₅ H ₅ F)	228.3
H(CHAl ₁₁ Cl ₅ H ₅ Cl)	230.0
H(CHAl ₁₁ F ₅ Cl ₅ H)	260.6
H(CHAl ₁₁ F ₅ Cl ₅ H)-O	248.9
H(CHAl ₁₁ F ₅ Cl ₅ F)	228.7
H(CHAl ₁₁ F ₅ Cl ₅ Cl)	234.8
H(CHAl ₁₁ Cl ₅ F ₅ H)	258.5
H(CHAl ₁₁ Cl ₅ F ₅ H)-O	250.4
H(CHAl ₁₁ Cl ₅ F ₅ F)	226.7
H(CHAl ₁₁ Cl ₅ F ₅ Cl)	231.3

Lewis acid, and associated X[−] ion affinities (ΔH_3) values for each Lewis acid.

We show these values with the species containing 10 H, 10 F, or 10 Cl atoms appearing first followed by species containing mixtures of 5 H, 5 F, or 5 Cl atoms. This ordering will be preserved in later tables and figures as we discuss acid strengths and molecular structures.

Two decades ago, Christie and co-workers proposed a quantitative scale for Lewis acidities based on fluoride ion affinities⁵⁴ introducing so-called pF[−] values obtained by taking the fluoride ion affinity in kcal/mol and dividing by 10. According to that scale, the strongest Lewis acid studied by Christie et al. was SbF₅ whose pF[−] was determined to be 12.03 (FIA = 120.3 kcal/mol). All of our Lewis acids based on the caralumane CAI₁₁ core have FIAs significantly exceeding 120 kcal/mol thus making them Lewis superacids. The two B-containing acids CHB₁₁F₅F₅ and CHB₁₁Cl₅Cl₅ have pF[−] values near 18. Even though the Lewis acids containing the carborane

CB₁₁ core are stronger than the acids with the CAI₁₁ core, the latter compounds still represent Lewis acids of higher acid strength than the systems commonly recognized as “strong Lewis acids” (e.g., AsF₅ (FIA = 105.9 kcal/mol), AlCl₃ (FIA = 114.6 kcal/mol), and AlF₃ (FIA = 115.0 kcal/mol)⁵⁴). The origin of such large FIAs is likely related to the nature of the LUMO orbitals of the Lewis acids, two of which are shown in Figure 1. There we see that electron density added to such a LUMO will be highly delocalized over the cage structure. We think it is the intrinsic electron binding energy of the B 2p or Al 3p orbital combined with significant stabilization due to delocalization that produces the large FIAs of these species.

3.2.2. Lewis Acid Structures. In Figure 6, we show the minimum-energy structures for the B- and Al-containing Lewis superacids considered here.

The Al-containing Lewis acids are significantly larger than the B-containing Lewis acids because the Al–Al separations (~2.7 Å) are larger than B–B separations (~1.8 Å), which makes the volume inside the caralumane CAI₁₁ core (ca. 43 Å³) approximately 3 times larger than the volume of carborane CB₁₁ core (ca. 13 Å³). Unlike the carborane CB₁₁ core, the caralumane CAI₁₁ core is not always icosahedral when the Lewis superacid is formed. In some cases (e.g., CHAl₁₁F₅F₅, CHAl₁₁Cl₅Cl₅, CHAl₁₁F₅H₅, CHAl₁₁Cl₅H₅, CHAl₁₁F₅Cl₅, and CHAl₁₁Cl₅F₅) its top and bottom sides are flattened as a result of which the whole structure adopts a quasi-antiprism shape rather than an icosahedron structure.

3.2.3. Brønsted Acid Structures. In Figures 7–10, we show the minimum-energy structures of the Brønsted superacids formed by adding HH, HF, or HCl to each of the Lewis superacids in Figure 6.

From Figures 7–10, we note that the formation of the Brønsted superacids H(CHAl₁₁X₅Y₅Z) causes the structures to adopt quasi-antiprism shapes in some cases. Analogous antiprism structures of the caralumane CAI₁₁ cores were noted earlier for some of the CHAl₁₁X₅Y₅ Lewis acids.

We also note that Z–H⋯F and Z–H⋯Cl hydrogen bonds are formed in the H(CHAl₁₁X₅F₅Z) and H(CHAl₁₁X₅Cl₅Z) superacids when Z = F or Cl, with the lengths of these H⋯F and H⋯Cl hydrogen bonds spanning a relatively wide range 1.369–2.865 Å (with the longest H-bond in H(CHAl₁₁F₅Cl₅Cl) depicted in Figure 10). In contrast, hydrogen bonds are absent (i) when H(CHAl₁₁X₅Y₅H) is formed upon the attachment of HH to CHAl₁₁X₅Y₅ (X, Y = F, Cl) (ii) when HH is attached to CHAl₁₁X₁₀ to form H(CHAl₁₁X₁₀)H (X = H, F, Cl) or (iii) when H(CHAl₁₁X₅H₅Z) is formed upon the attachment of HZ to CHAl₁₁X₅H₅ (X = F, Cl). In case iii, the hydrogen bonds do not form because H atoms occupy the ortho-belt positions; only when ortho-belt positions are occupied by F or Cl atoms do hydrogen bonds form.

In cases i and ii, the attachment of HH leads to Brønsted superacid structures of both the non-O and O type neither of which possess hydrogen bonds. In the non-O structures, the HH moiety is oriented horizontally above the top Al atom of the CAI₁₁ core. The equal Al–H separations between the top Al atom and each of H atoms and the short (0.75–0.78 Å) H–H separation (close to that in H₂) suggests that H(CHAl₁₁X₅Y₅H) or H(CHAl₁₁X₁₀H) can be treated as CHAl₁₁X₅Y₅ or CHAl₁₁X₁₀ with the H₂ molecule tethered to it serving as a Lewis base. Because HH has no lone-pair electrons available to donate, this suggests that HH uses its two σ -bonding electrons to donate into the vacant 3p orbital of Al atom and does so in a manner that can be denoted η^2 -H₂.

Table 3. Enthalpies (kcal/mol) for Binding HX to Lewis acid LA ($-\Delta H_1$), Deprotonating the Lewis–Brønsted acid (ΔH_2), and Removing X^- from LAX^- (ΔH_3), EA of X, IP of H, and D_e of HX^a

Lewis–Brønsted superacid	$-\Delta H_1$	ΔH_2	ΔH_3	EA_X	IP_H	$D_e(HX)$	$\Delta H_2 + \Delta H_3 + EA_X - IP_H - D_e(HX)$
H(CHAl ₁₁ H ₃ H ₃ H)	4.77	269.38	134.19	7.92	313.34	93.37	4.77
H(CHAl ₁₁ H ₃ H ₃ H)-O	14.25	278.86	134.19	7.92	313.34	93.37	14.25
H(CHB ₁₁ H ₃ H ₃ H)	18.51	266.86	150.44	7.92	313.34	93.37	18.51
H(CHB ₁₁ H ₃ H ₃ H)-O	14.04	262.39	150.44	7.92	313.34	93.37	14.04
H(CHAl ₁₁ H ₃ H ₃ F)	12.19	242.65	134.72	81.73	313.34	133.59	12.19
H(CHAl ₁₁ H ₃ H ₃ Cl)	12.78	243.62	97.72	81.96	313.34	97.18	12.78
H(CHAl ₁₁ F ₃ F ₃ H)	1.45	265.00	135.24	7.92	313.34	93.37	1.45
H(CHAl ₁₁ F ₃ F ₃ H)-O	-7.58	255.97	135.24	7.92	313.34	93.37	-7.58
H(CHAl ₁₁ F ₃ F ₃ F)	6.86	239.46	132.59	81.73	313.34	133.59	6.86
H(CHB ₁₁ F ₃ F ₃ F)	38.04	224.57	178.67	81.73	313.34	133.59	38.04
H(CHAl ₁₁ F ₃ F ₃ Cl)	7.71	240.64	95.63	81.96	313.34	97.18	7.71
H(CHAl ₁₁ Cl ₃ Cl ₃ F)	11.26	232.68	143.78	81.73	313.34	133.59	11.26
H(CHAl ₁₁ Cl ₃ Cl ₃ H)	3.65	255.87	146.58	7.92	313.34	93.37	3.65
H(CHAl ₁₁ Cl ₃ Cl ₃ H)-O	1.30	253.52	146.58	7.92	313.34	93.37	1.30
H(CHAl ₁₁ Cl ₃ Cl ₃ Cl)	11.98	233.38	107.15	81.96	313.34	97.18	11.98
H(CHB ₁₁ Cl ₃ Cl ₃ Cl)	52.78	235.10	146.24	81.96	313.34	97.18	52.78
H(CHAl ₁₁ H ₃ F ₃ H)	6.46	259.62	145.63	7.92	313.34	93.37	6.46
H(CHAl ₁₁ H ₃ F ₃ H)-O	15.87	269.04	145.63	7.92	313.34	93.37	15.87
H(CHAl ₁₁ H ₃ F ₃ F)	22.13	242.50	144.82	81.73	313.34	133.59	22.13
H(CHAl ₁₁ H ₃ F ₃ Cl)	20.46	241.58	185.56	107.44	313.34	97.18	20.46

^aIn the last column is the sum $\Delta H_2 + \Delta H_3 + EA_X - IP_H - D_e(HX)$, which should equal $-\Delta H_1$, as it does. We remind the reader that we employed ΔH values for the EAs, IP, and D_e s when constructing the data shown here.

Table 4. Enthalpies (kcal/mol) for Binding HX to Lewis Acid LA ($-\Delta H_1$), Deprotonating the Lewis–Brønsted Acid (ΔH_2), and Removing X^- from LAX^- (ΔH_3), EA of X, IP of H, and D_e of HX^a

Lewis–Brønsted superacid	$-\Delta H_1$	ΔH_2	ΔH_3	EA_X	IP_H	$D_e(HX)$	$\Delta H_2 + \Delta H_3 + EA_X - IP_H - D_e(HX)$
H(CHAl ₁₁ F ₃ H ₃ H)	1.46	264.37	135.88	7.92	313.34	93.37	1.46
H(CHAl ₁₁ F ₃ H ₃ H)-O	3.64	266.55	135.88	7.92	313.34	93.37	3.64
H(CHAl ₁₁ F ₃ H ₃ F)	3.71	234.97	133.94	81.73	313.34	133.59	3.71
H(CHAl ₁₁ F ₃ H ₃ Cl)	5.65	236.81	97.40	81.96	313.34	97.18	5.65
H(CHAl ₁₁ H ₃ Cl ₃ H)	7.41	256.87	149.33	7.92	313.34	93.37	7.41
H(CHAl ₁₁ H ₃ Cl ₃ H)-O	15.82	265.28	149.33	7.92	313.34	93.37	15.82
H(CHAl ₁₁ H ₃ Cl ₃ F)	23.41	240.30	148.30	81.73	313.34	133.59	23.41
H(CHAl ₁₁ H ₃ Cl ₃ Cl)	23.45	240.80	111.20	81.96	313.34	97.18	23.45
H(CHAl ₁₁ Cl ₃ H ₃ H)	0.91	257.35	142.35	7.92	313.34	93.37	0.91
H(CHAl ₁₁ Cl ₃ H ₃ H)-O	8.53	264.97	142.35	7.92	313.34	93.37	8.53
H(CHAl ₁₁ Cl ₃ H ₃ F)	4.34	228.71	140.82	81.73	313.34	133.59	4.34
H(CHAl ₁₁ Cl ₃ H ₃ Cl)	9.15	233.64	104.06	81.96	313.34	97.18	9.15
H(CHAl ₁₁ F ₃ Cl ₃ H)	2.39	260.89	140.28	7.92	313.34	93.37	2.39
H(CHAl ₁₁ F ₃ Cl ₃ H)-O	-4.69	253.82	140.28	7.92	313.34	93.37	-4.69
H(CHAl ₁₁ F ₃ Cl ₃ F)	6.40	234.37	137.23	81.73	313.34	133.59	6.40
H(CHAl ₁₁ F ₃ Cl ₃ Cl)	9.77	237.53	100.80	81.96	313.34	97.18	9.77
H(CHAl ₁₁ Cl ₃ F ₃ H)	1.55	258.08	142.26	7.92	313.34	93.37	1.55
H(CHAl ₁₁ Cl ₃ F ₃ H)-O	-1.11	255.42	142.26	7.92	313.34	93.37	-1.11
H(CHAl ₁₁ Cl ₃ F ₃ F)	7.98	233.47	139.70	81.73	313.34	133.59	7.98
H(CHAl ₁₁ Cl ₃ F ₃ Cl)	7.98	233.94	102.60	81.96	313.34	97.18	7.98

^aIn the last column is the sum $\Delta H_2 + \Delta H_3 + EA_X - IP_H - D_e(HX)$, which should equal $-\Delta H_1$, as it does. We remind the reader that we employed ΔH values for the EAs, IP, and D_e s when constructing the data shown here.

Alternatively, in cases i and ii, the attachment of HH can lead to O-type structures in which the HH molecule is cleaved heterolytically to generate a hydride anion that bonds to the antipodal Al atom and a proton that bonds to the antipodal Al and within the ortho-belt. Again, no hydrogen bonds occur in these cases. In fact, there are also O-type structures in which the proton is bonded between the ortho- and meta-belt locations. The former of these O-type and the non-O type structures appear in Figures 7–10.

3.2.4. Brønsted Acid Strengths. In Table 2, we show the acid strength data obtained for the multitude of Brønsted acids studied here. Recall that the species labeled with O are those in which the HH Lewis base is cleaved upon addition to the Lewis acid to form the Brønsted acid. The corresponding Brønsted acid in which the HH molecule serves as a Lewis base but remains essentially intact is not labeled with O.

Because all of these species have $\Delta G_a^{298} < 303$ kcal/mol, they all can be called Brønsted superacids. Among them, it

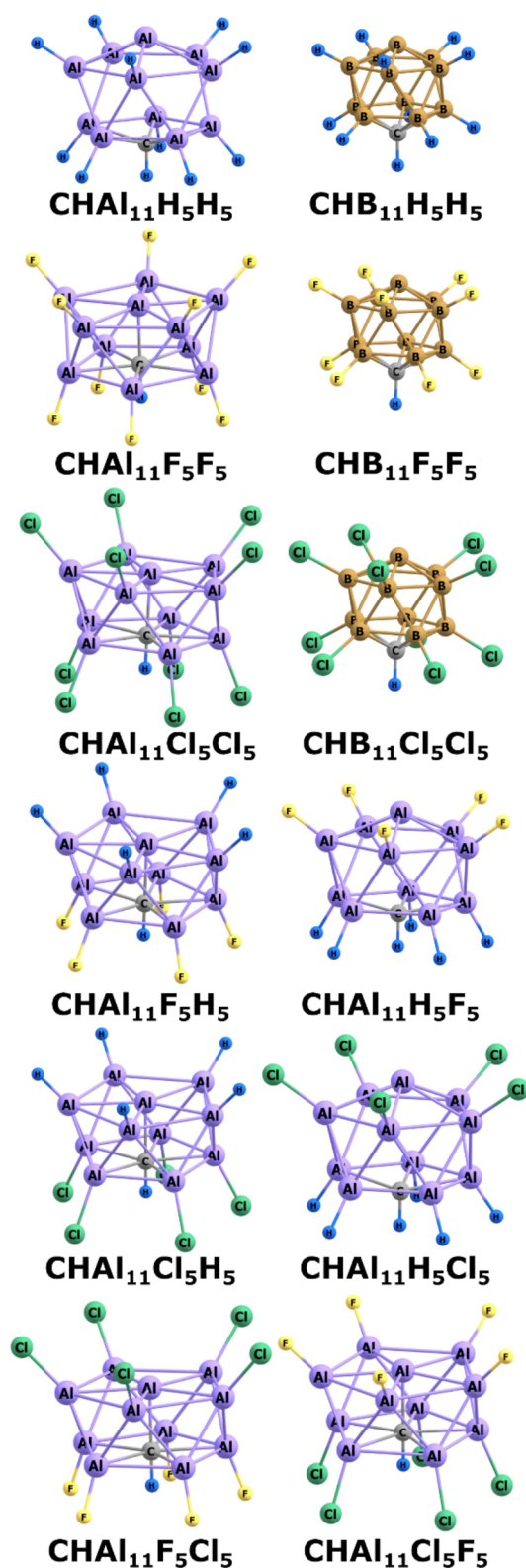


Figure 6. Equilibrium structures of Lewis acids.

appears that H(CHB₁₁F₅F₅) is the strongest, but several others are close in acid strength. Also it seems that the Al-containing molecules are usually a bit weaker acids than the corresponding B-containing molecules as they have larger ΔG_a^{298} values. The largest Gibbs free deprotonation energy of 273.2 kcal/mol (i.e., corresponding to the weakest acid) was

found for the caralumane acid containing only hydrogen atoms as substituents H(CHAl₁₁H₅H₅)₂O. In general, the carborane and caralumane acids containing a large number of H atoms correspond to weaker acids (among the systems studied) having ΔG_a^{298} values that exceed 250 kcal/mol (but below 303 kcal/mol, still making them superacids). The acid strengths of the carborane and caralumane Brønsted superacids gathered in Table 2 are comparable to those of variously substituted carborane acids reported by Lipping et al.⁴⁵ and appreciably larger than the strength of organometallic superacids based on sulfonic acid derivatives containing $-BX_2$ (X = H, F, Cl, Br) electron-pair acceptor group described by Valadbeigi and Gal⁵⁵ or $BX_3H_2SO_4$ and $(BX_3)_2H_2SO_4$ (X = H, F, Cl, Br, CN, OH) Lewis–Brønsted superacids studied by Valadbeigi and Kurtén.⁵⁶

Although the caralumane superacids appear to be slightly weaker acids than the carborane superacids, the formers' strengths seem to be similar, which makes them a promising group of compounds to explore synthesizing as they would likely exhibit analogous properties to the systems based on a CB₁₁ carborane core.

3.2.5. Connections between Lewis and Brønsted Acid Strengths. Earlier, we pointed out how the enthalpy changes for attaching a Lewis base to a Lewis acid (ΔH_1), for deprotonating the resulting Brønsted acid (ΔH_2), and for removing the X[−] anion from the conjugate base of the Brønsted acid (ΔH_3) could be interconnected via the thermodynamic cycle shown in Figure 5. In Tables 3 and 4, we illustrate these interconnections for the Lewis–Brønsted superacids studied here.

It is worth noting that the $-\Delta H_1$ values listed in Tables 3 and 4 for the Brønsted acids labeled O do not represent enthalpy changes for simply attaching an HH molecule as a Lewis base to the corresponding Lewis acid. As explained earlier, in these cases, the HH molecule is cleaved and the two H atoms end up bonded to different sites; one as a hydride ion and the other as a proton. For example, the $-\Delta H_1$ value shown for H(CHAl₁₁F₅F₅H) O is even negative (−7.58 kcal/mol), meaning that it is endothermic to add HH to (CHAl₁₁F₅F₅). It is also worth noting that the $-\Delta H_1$ values associated with the HH adducts labeled O are sometimes larger than those associated with the corresponding HH adducts not labeled O. This means that for some of the Brønsted superacids, the O compound is more stable while for others the compound not labeled O is more stable. Specifically,

- H(CHB₁₁H₅H₅H)₂O is less stable than H(CHB₁₁H₅H₅H) by 4.64 kcal/mol,
- H(CHAl₁₁H₅H₅H) is less stable than H(CHAl₁₁H₅H₅H)₂O by 9.03 kcal/mol,
- H(CHAl₁₁F₅F₅H)₂O is less stable than H(CHAl₁₁F₅F₅H) by 8.98 kcal/mol,
- H(CHAl₁₁Cl₅Cl₅H)₂O is less stable than H(CHAl₁₁Cl₅Cl₅H) by 0.96 kcal/mol,
- H(CHAl₁₁H₅Cl₅H) is less stable than H(CHAl₁₁H₅Cl₅H)₂O by 7.61 kcal/mol,
- H(CHAl₁₁Cl₅H₅H) is less stable than H(CHAl₁₁Cl₅H₅H)₂O by 7.09 kcal/mol,
- H(CHAl₁₁F₅H₅H) is less stable than H(CHAl₁₁F₅H₅H)₂O by 2.58 kcal/mol, and
- H(CHAl₁₁H₅F₅H) is less stable than H(CHAl₁₁H₅F₅H)₂O by 8.67 kcal/mol.

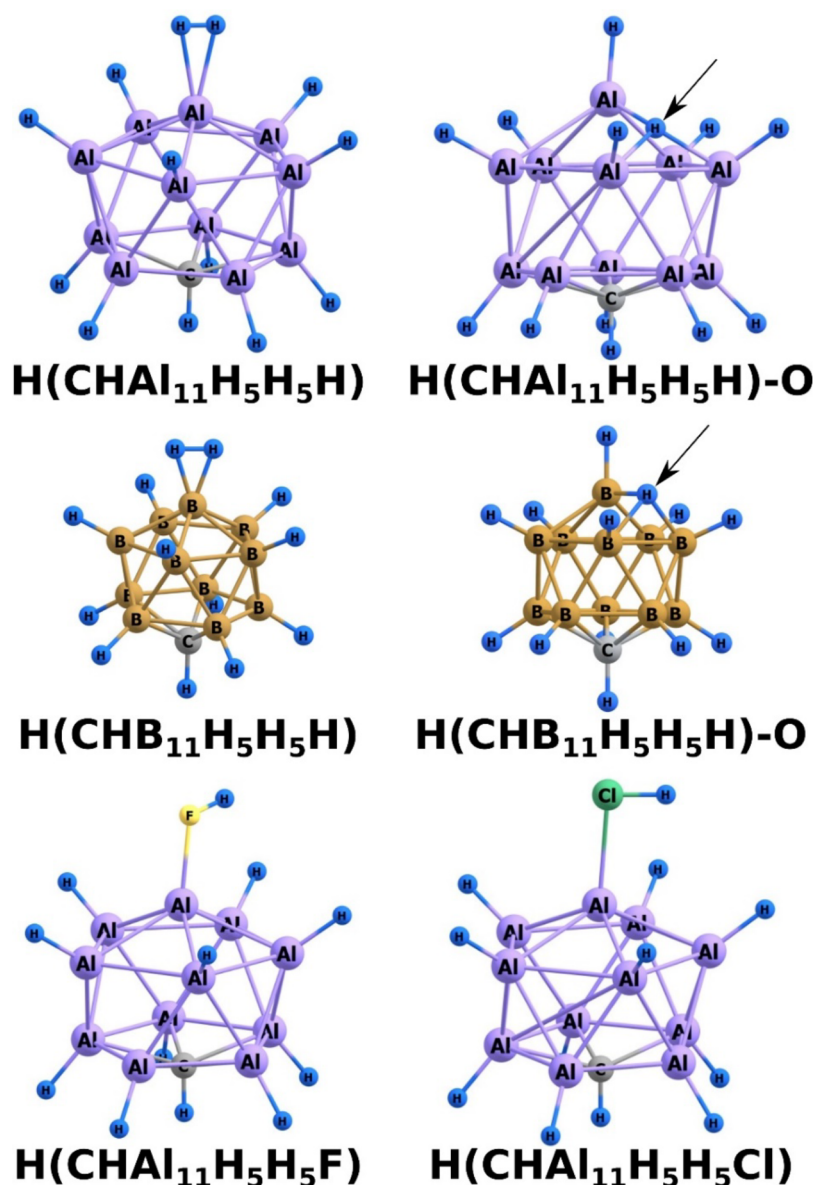


Figure 7. Equilibrium structures of Brønsted acids with H atoms in all ortho- and meta-belt positions.

Finally, it is interesting to note that although the enthalpy gained when binding HH to any of the Lewis acids ($-\Delta H_1$) can be quite small, the resulting $\text{H}(\text{CHAl}_{11}\text{X}_5\text{Y}_5\text{H})$ and $\text{H}(\text{CHB}_{11}\text{X}_5\text{Y}_5\text{H})$ Brønsted acids are still very strong (see Table 2). This observation is in line with noting that the H^- affinities of $(\text{CHAl}_{11}\text{X}_5\text{Y}_5)$ and $(\text{CHB}_{11}\text{X}_5\text{Y}_5)$ are large as the fourth columns in Tables 3 and 4 affirm.

3.2.6. Conversions between O- and Non-O Brønsted Acids. Earlier, it was shown that when HH acts as the Lewis base and adds to one of our Lewis acids to form a Brønsted acid, there are two distinct structures that can be formed and that these structures can have similar energies. In Figure 11, we show intrinsic reaction path (IRP) energy profiles for two such cases $\text{H}(\text{CHAl}_{11}\text{H}_{10}\text{H})$ and $\text{H}(\text{CHB}_{11}\text{H}_{10}\text{H})$ with the horizontal axis being the distance in Å between the two H atoms in the HH Lewis base.

In these profiles, we show on the left the energies of the non-O isomer as the reference energy because the formation of this isomer from HH and the Lewis acid proceeds in a thermochemically downhill manner (22.5 kcal/mol for H-

$(\text{CHB}_{11}\text{H}_5\text{H}_5\text{H})$ and 6.5 kcal/mol for $\text{H}(\text{CHAl}_{11}\text{H}_5\text{H}_5\text{H})$) with no intervening barrier. In attempting to characterize paths forming the O isomers directly from HH and the Lewis acid, we were unable to identify any low-energy direct path; it appears that the lowest-energy route to forming these isomers is to first form the non-O isomer and to then cross the transition state (TS1 in Figure 11) to the O isomer.

The energies of TS1 correspond to those of the transition states connecting the non-O and O-type structures with the latter having the proton bonded between the antipodal Al and two ortho-belt Al atoms. It turns out that for the O-type structures in which the proton is so located, it is possible for the H^+ to migrate to a position in which it is bound between the ortho- and meta- belts as shown in Figure 12. This alternative O-type species is labeled II in Figure 11, where one can see that its energy can be comparable to that of the O-type species in which the proton resides between the antipodal Al and two ortho-belt Al atoms. The energies labeled TS2 correspond to those of the transition states connecting these two different O-type isomers.

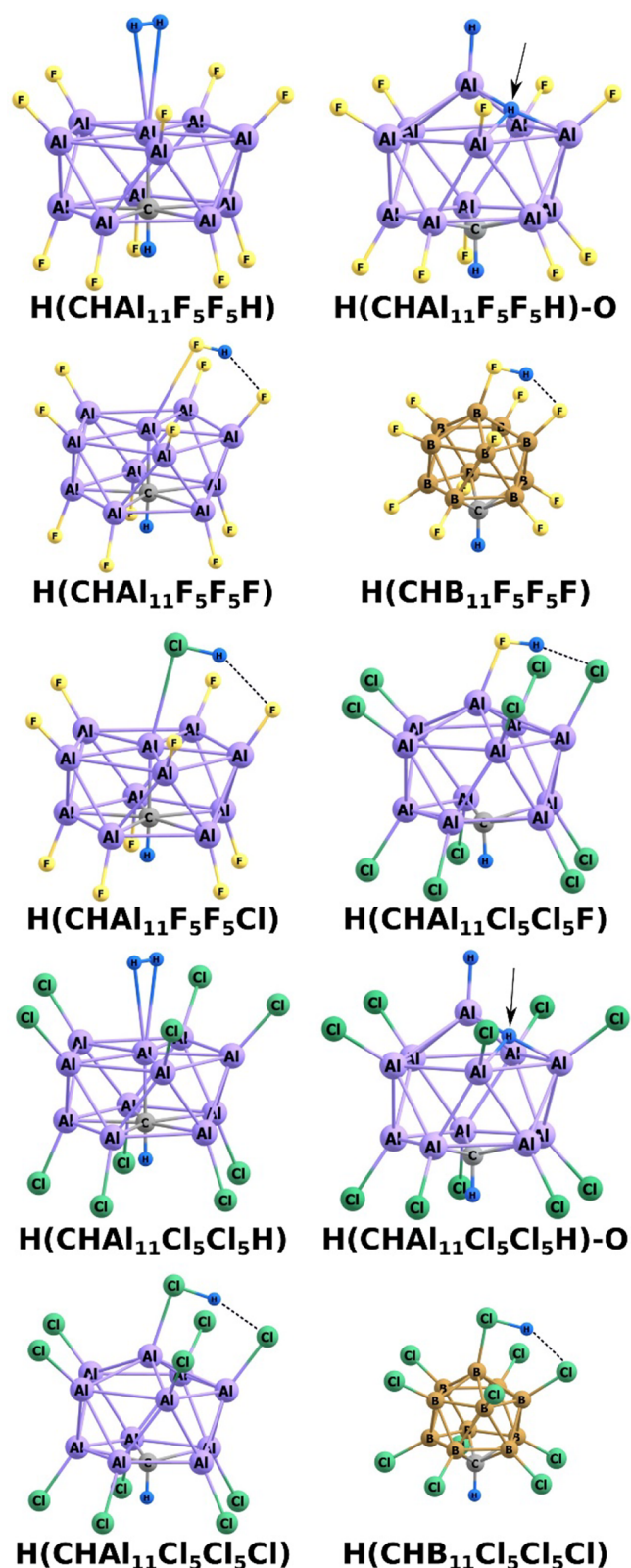


Figure 8. Equilibrium structures of Brønsted acids with all Cl or all F atoms in ortho- and meta-belt positions.

These two examples illustrate what we said earlier about the relative energies of the O-type and non-O structures; their relative energies are not always in the same order but vary within the compounds studied here. The examples also show that the barriers between the O- and non-O structures can be

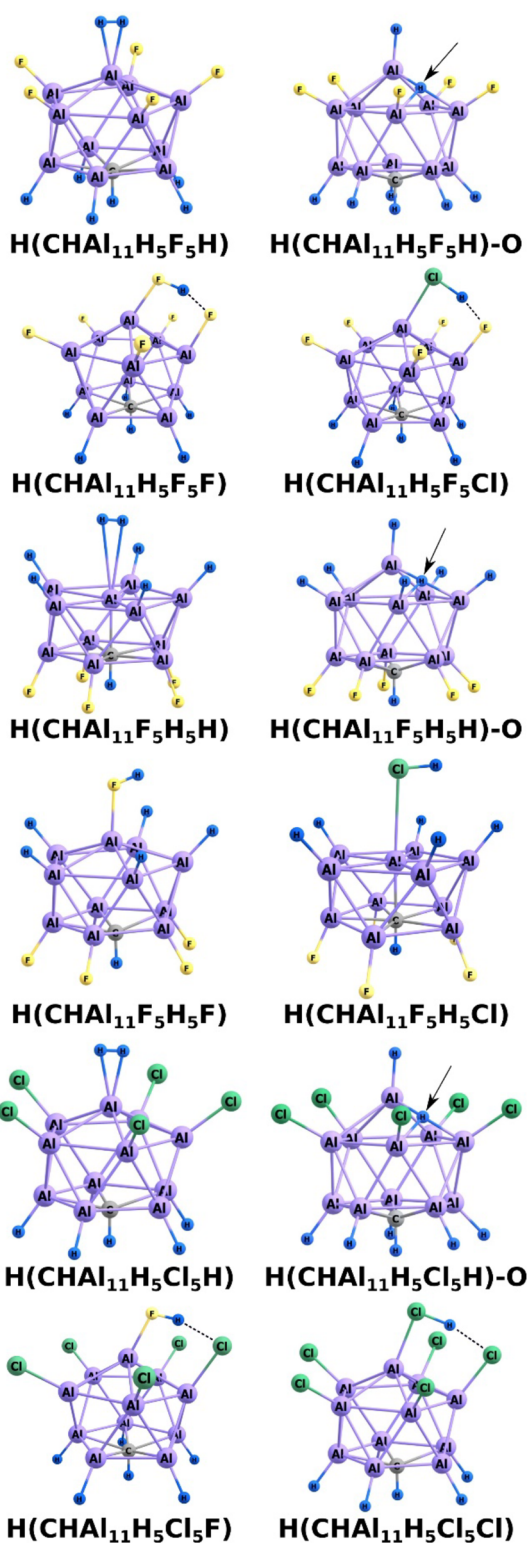


Figure 9. Equilibrium structures of Brønsted acid with mixed ortho- and meta-belt ligands.

large enough for the higher-energy structure to be kinetically stable at room temperature. The barriers connecting the two types (I and II) of O-type species appear to be lower but high enough to make these structures not fluxional near room temperatures.

3.2.7. Conversions between Equivalent O-Type Brønsted Acid Structures. It is also possible for an O-type Brønsted acid

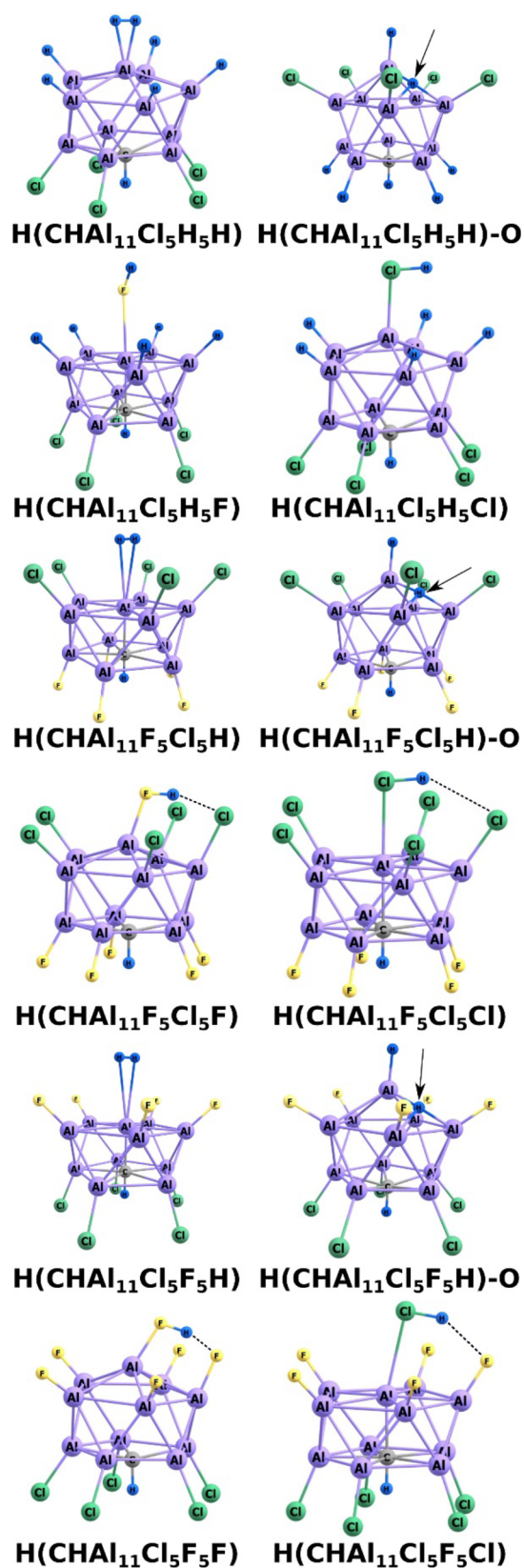


Figure 10. Equilibrium structures of Bronsted acid with mixed ortho- and meta-belt ligands.

to undergo isomerization in which the proton migrates from one ortho-belt position to another ortho-belt position having equal energy. We found the barriers for this isomerization to be

3.7 kcal/mol for H(CHB₁₁H₅H₅H)-O and 9.6 kcal/mol for H(CHAl₁₁H₅H₅H)-O as shown in Figures 13 and 14, where we show the corresponding reaction path energy profiles for these two species in which the horizontal is the distance along the intrinsic reaction coordinate (IRC).

In Figures 15 and 16, we show the transition-state structures for converting between two energy-equivalent O-structures for the H(CHB₁₁H₅H₅H) and H(CHAl₁₁H₅H₅H) cases, respectively.

Finally, we should note that there exist alternative paths connecting the pairs of energy equivalent ortho-belt O-type structures discussed above, but these paths have higher barriers. For example, one O-type H(CHAl₁₁H₅H₅H) can first undergo conversion to its corresponding non-O structure; this step requires ca. 28 kcal/mol as Figure 11 illustrates (for H(CHB₁₁H₅H₅H) the corresponding barrier is 5.5 kcal/mol). Next, the non-O structure can undergo a rearrangement in which the HH fragment attached to the antipodal Al or B atom rotates to an energetically equivalent orientation as shown in Figure 17; we found the barrier to such rotations to be extremely small (<0.1 kcal/mol) for both H(CHAl₁₁H₅H₅H) and H(CHB₁₁H₅H₅H), so this motion is essentially free.

After coming to a new orientation, this non-O species could then surmount the non-O to O-type barrier (ca. 18 kcal/mol for H(CHAl₁₁H₅H₅H) and ca. 11 kcal/mol for H(CHB₁₁H₅H₅H) as shown in Figure 11) to form the new energy-equivalent ortho-belt O structure.

4. CONCLUSIONS

Analogues of carborane superacids in which the CB₁₁ carborane core is replaced by a CA₁₁ core have been studied using ab initio electronic structure tools. A wide variety of caralumane Brønsted superacids H(CHAl₁₁X₅Y₅Z) with X, Y, and Z = F, Cl, or H are shown to be formed by adding HF, HCl, or HH to a corresponding caralumane Lewis superacid CHAl₁₁X₅Y₅. The F⁻ ion affinities of the CHAl₁₁X₅Y₅ Lewis acids all substantially exceed 120 kcal/mol thus making them Lewis superacids. The deprotonation Gibbs free energies of the H(CHAl₁₁X₅Y₅Z) are all less than 303 kcal/mol which makes them all Brønsted superacids. When HF or HCl is bound to a caralumane Lewis acid to form the Brønsted acid, the halogen atom of HF or HCl is bound datively to the antipodal Al atom. Then, if there are F or Cl atoms bonded to ortho-belt Al atoms, a hydrogen bond is formed between the HF or HCl molecule's H atom and an ortho-belt F or Cl atom. Two examples of such a structural motif appear in Figure 4. If the ortho-belt Al atoms have no halogen atoms attached, then no hydrogen bond is formed with the HF or HCl molecule's H atom.

Interestingly, when HH is bound to the Lewis acid to form the Brønsted acid, two very different structures arise although both still display Brønsted superacid characteristics. In the structures labeled non-O in this text, an essentially intact HH molecule is datively bound to the antipodal Al atom but in a η² manner in which the HH molecule donates its σ² electron pair into the antipodal Al atom's vacant 3p orbital. In the structures labeled O-type, the HH molecule is heterolytically cleaved to generate a hydride ion that attaches to the antipodal Al atom and a proton that binds either in a multicenter manner to the antipodal Al and to two ortho-belt Al atoms or to Al atoms in the ortho- and meta-belts. Figure 3 shows examples of the O-type and non-O structures for one of the boron-containing cases studied here. The O-type and non-O structures are connected by a reaction path along which a substantial energy

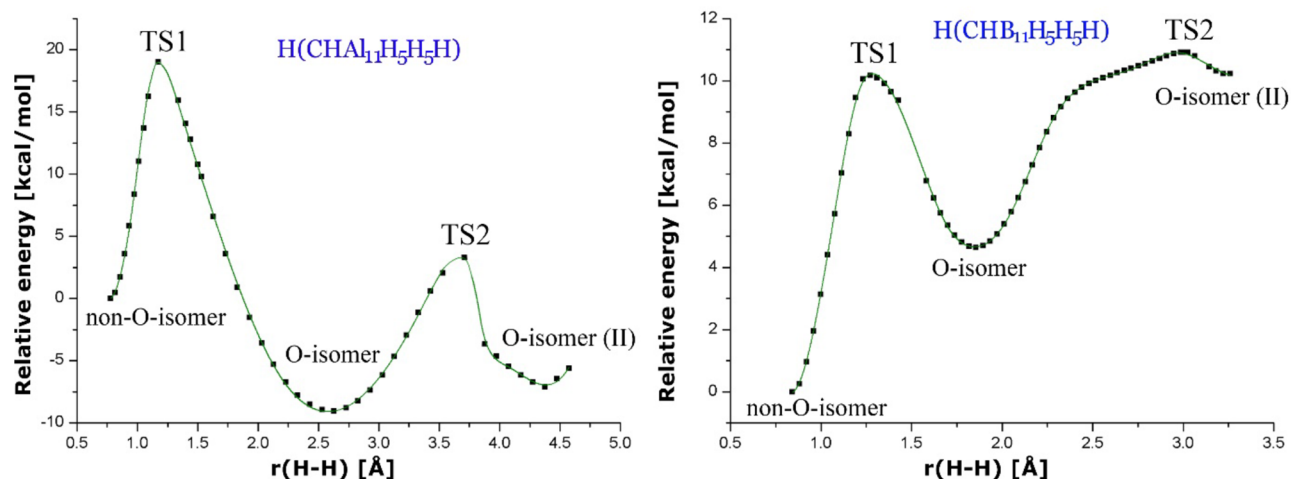


Figure 11. Energy profiles leading from non-O isomer ($\text{H}(\text{CHAl}_{11}\text{H}_5\text{H}_5\text{H})$, left; $\text{H}(\text{CHB}_{11}\text{H}_5\text{H}_5\text{H})$, right) over a transition state (TS1) to a corresponding O-type isomer (labeled I) with the proton located near the antipodal Al and two ortho-belt Al atoms. From that O-type isomer (labeled I) a path leads over TS2 to a different O-type isomer (labeled II) with the proton between the ortho- and meta-belts.

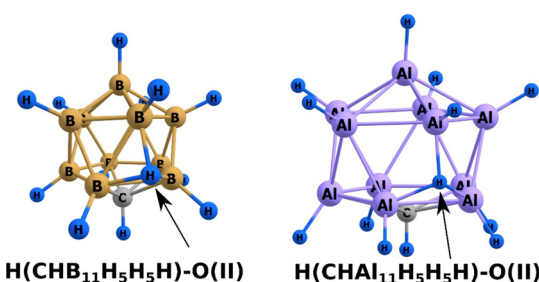


Figure 12. Equilibrium structures of alternative O-type isomers of $\text{H}(\text{CHB}_{11}\text{H}_5\text{H}_5\text{H})$ and $\text{H}(\text{CHAl}_{11}\text{H}_5\text{H}_5\text{H})$ with the proton between ortho- and meta-belts (labeled II in Figure 11).

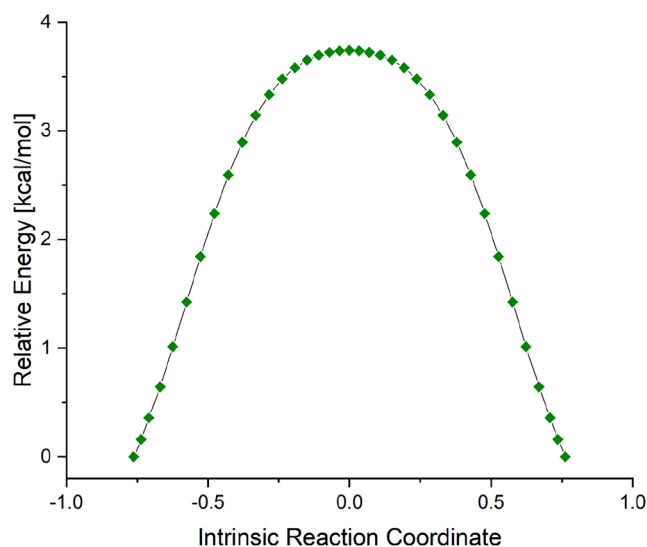


Figure 13. IRC path connecting two energy-equivalent O-isomers of $\text{H}(\text{CHB}_{11}\text{H}_5\text{H}_5\text{H})$.

barrier occurs as illustrated in Figure 11. This suggests that they could both be kinetically stable near room temperature. Moreover, in the ortho-belt O-type structures, the proton can migrate to a meta-belt position to form a second class of O-type species as also shown in Figure 11 but must overcome an energy barrier to do so. Finally, as illustrated in Figures 13 and

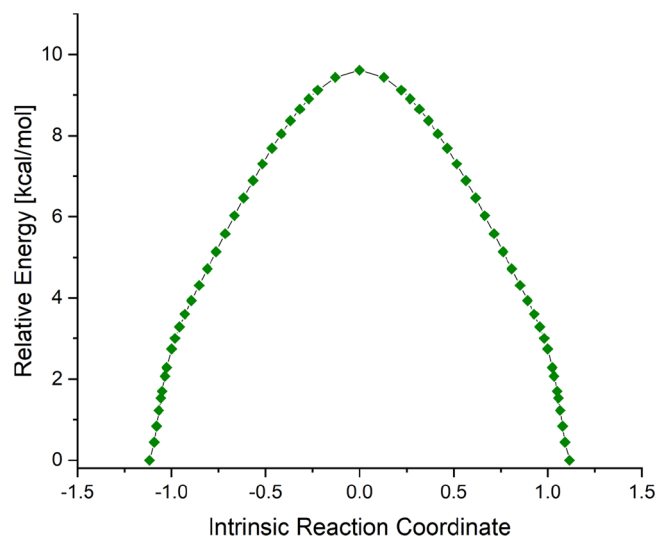


Figure 14. IRC path connecting two energy-equivalent O-isomers of $\text{H}(\text{CHAl}_{11}\text{H}_5\text{H}_5\text{H})$.

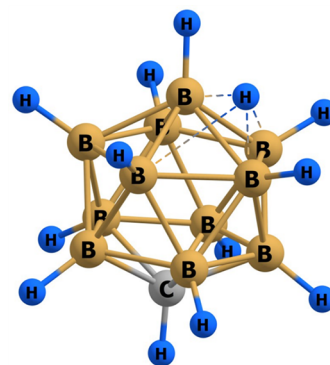


Figure 15. Transition state structure for $\text{H}(\text{CHB}_{11}\text{H}_5\text{H}_5\text{H})\text{-O} \rightarrow \text{H}(\text{CHB}_{11}\text{H}_5\text{H}_5\text{H})\text{-O}$.

14, an ortho-belt O-type species can isomerize to a degenerate structure by overcoming a barrier of ca. 3.5 kcal/mol, suggesting that these species could be somewhat fluxional.

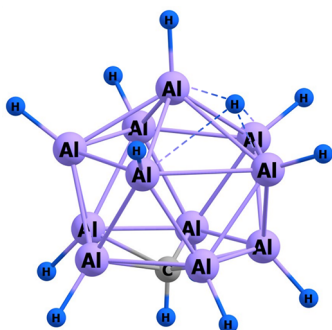


Figure 16. Transition state structure for $\text{H}(\text{CHAl}_{11}\text{H}_5\text{H}_3\text{H})\text{-O} \rightarrow \text{H}(\text{CHAl}_{11}\text{H}_5\text{H}_3\text{H})\text{-O}$.

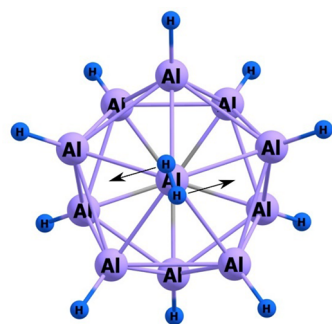


Figure 17. TS structure for the rotation of the H_2 fragment.

■ ASSOCIATED CONTENT

Supporting Information

The Supporting Information is available free of charge at <https://pubs.acs.org/doi/10.1021/acs.jpca.0c11014>.

Cartesian coordinates of the stationary-point structures (i.e., local minima and transition states) (PDF)

■ AUTHOR INFORMATION

Corresponding Author

Jack Simons – Henry Eyring Center for Theoretical Chemistry, Department of Chemistry, University of Utah, Salt Lake City, Utah 84112, United States; orcid.org/0000-0001-8722-184X; Email: jack.simons@utah.edu

Authors

Jakub Brzeski – Laboratory of Quantum Chemistry, Faculty of Chemistry, University of Gdańsk, 80-308 Gdańsk, Poland; orcid.org/0000-0003-4865-0152

Piotr Skurski – Laboratory of Quantum Chemistry, Faculty of Chemistry, University of Gdańsk, 80-308 Gdańsk, Poland; Henry Eyring Center for Theoretical Chemistry, Department of Chemistry, University of Utah, Salt Lake City, Utah 84112, United States; orcid.org/0000-0002-2091-6193

Complete contact information is available at: <https://pubs.acs.org/10.1021/acs.jpca.0c11014>

Notes

The authors declare no competing financial interest.

■ ACKNOWLEDGMENTS

This research was supported by the Polish Ministry of Science and Higher Education Grant No. DS 531-T110-D499-20 (to P.S.). The calculations have been carried out using resources

provided by the Wrocław Centre for Networking and Supercomputing (<http://wcss.pl>), Grant No. 455.

■ REFERENCES

- (1) Mallouk, T. E.; Rosenthal, G. L.; Mueller, G.; Brusasco, R.; Bartlett, N. Fluoride Ion Affinities of Germanium Tetrafluoride and Boron Trifluoride from Thermodynamic and Structural Data for $(\text{SF}_3)_2\text{GeF}_6$, ClO_2GeF_5 , and ClO_2BF_4 . *Inorg. Chem.* **1984**, *23* (20), 3167–3173.
- (2) Krossing, I.; Raabe, I. Relative Stabilities of Weakly Coordinating Anions: A Computational Study. *Chem. - Eur. J.* **2004**, *10* (20), 5017–5030.
- (3) Kögel, J. F.; Timoshkin, A. Y.; Schröder, A.; Lork, E.; Beckmann, J. $\text{Al}(\text{OCARF}_3)_3$ – a Thermally Stable Lewis Superacid. *Chem. Sci.* **2018**, *9* (43), 8178–8183.
- (4) Saeidian, H.; Shams, B.; Mirjafary, Z. Comprehensive DFT Calculations on Organic Sulfuric Acid Derivatives to Design of Powerful Neutral Organic Superacids. *Struct. Chem.* **2019**, *30*, 787.
- (5) Valadbeigi, Y.; Vianello, R. A Density Functional Theory Study on the Superacidity of Sulfuric, Fluorosulfuric, and Triflic Acid Derivatives with Two Cyclopentadiene Rings: Ion Pairs Formation in the Gas Phase. *J. Phys. Org. Chem.* **2019**, *32* (10), e3995.
- (6) Viggiano, A. A.; Henchman, M. J.; Dale, F.; Deakynne, C. A.; Paulson, J. F. Gas-Phase Reactions of Weak Brønsted Bases I^- , PO_3^- , HSO_4^- , FSO_3^- , and CF_3SO_3^- with Strong Brønsted Acids H_2SO_4 , FSO_3H , and $\text{CF}_3\text{SO}_3\text{H}$. A Quantitative Intrinsic Superacidity Scale for the Sulfonic Acids XSO_3H ($\text{X} = \text{HO}, \text{F}, \text{and } \text{CF}_3$). *J. Am. Chem. Soc.* **1992**, *114*, 4299.
- (7) Jelinek, T.; Baldwin, P.; Scheidt, W. R.; Reed, C. A. New Weakly Coordinating Anions. 2. Derivatization of the Carborane Anion $\text{CB}_{11}\text{H}_{12}^-$. *Inorg. Chem.* **1993**, *32* (10), 1982–1990.
- (8) Olaru, M.; Hesse, M. F.; Rychagova, E.; Ketkov, S.; Mebs, S.; Beckmann, J. The Weakly Coordinating Tris(Trichlorosilyl)Silyl Anion. *Angew. Chem., Int. Ed.* **2017**, *56* (52), 16490–16494.
- (9) Gutsev, G. L.; Boldyrev, A. I. DVM- α Calculations on the Ionization Potentials of MX_{k+1}^- Complex Anions and the Electron Affinities of MX_{k+1} “Superhalogens”. *Chem. Phys.* **1981**, *56* (3), 277–283.
- (10) Gutsev, G. L.; Boldyrev, A. I. DVM α Calculations on the Electronic Structure of Complex Chlorine Anions. *Chem. Phys. Lett.* **1981**, *84* (2), 352–355.
- (11) Gutsev, G. L.; Boldyrev, A. I. An Explanation of the High Electron Affinities of the 5d-Metal Hexafluorides. *Chem. Phys. Lett.* **1983**, *101* (4–5), 441–445.
- (12) Gutsev, G. L.; Boldyrev, A. I. The Way to Systems with the Highest Possible Electron Affinity. *Chem. Phys. Lett.* **1984**, *108* (3), 250–254.
- (13) Gutsev, G. L.; Boldyrev, A. I. The Relationship between the Electronic Structures of the 3d and 4d Metal Tetraoxanions and the Electron Affinities of the Corresponding Neutrals. *Chem. Phys. Lett.* **1984**, *108* (3), 255–258.
- (14) Gutsev, G. L.; Boldyrev, A. I. The Electronic Structure of the 3 and 4 d Metal Hexafluoride Anions and the Electron Affinities of the Corresponding Neutrals. *Mol. Phys.* **1984**, *53* (1), 23–31.
- (15) Gutsev, G. L.; Boldyrev, A. I. The Electronic Structure of Superhalogens and Superalkalies. *Russ. Chem. Rev.* **1987**, *56* (6), 519–531.
- (16) Gutsev, G. L.; Bartlett, R. J.; Boldyrev, A. I.; Simons, J. Adiabatic Electron Affinities of Small Superhalogens: LiF_2 , LiCl_2 , NaF_2 , and NaCl_2 . *J. Chem. Phys.* **1997**, *107* (10), 3867–3875.
- (17) Wang, X.-B.; Ding, C.-F.; Wang, L.-S.; Boldyrev, A. I.; Simons, J. First Experimental Photoelectron Spectra of Superhalogens and Their Theoretical Interpretations. *J. Chem. Phys.* **1999**, *110* (10), 4763–4771.
- (18) Armand, M.; Johansson, P. Novel Weakly Coordinating Heterocyclic Anions for Use in Lithium Batteries. *J. Power Sources* **2008**, *178* (2), 821–825.

- (19) Drent, E.; Arnoldy, P.; Budzelaar, P. H. M. Efficient Palladium Catalysts for the Carbonylation of Alkynes. *J. Organomet. Chem.* **1993**, *455* (1–2), 247–253.
- (20) Arndt, S.; Okuda, J. Cationic Alkyl Complexes of the Rare-Earth Metals: Synthesis, Structure, and Reactivity. *Adv. Synth. Catal.* **2005**, *347* (2–3), 339–354.
- (21) Armand, M.; Johansson, P. Novel Weakly Coordinating Heterocyclic Anions for Use in Lithium Batteries. *J. Power Sources* **2008**, *178* (2), 821–825.
- (22) Krossing, I.; Raabe, I. Noncoordinating Anions—Fact or Fiction? A Survey of Likely Candidates. *Angew. Chem., Int. Ed.* **2004**, *43* (16), 2066–2090.
- (23) Honeychuck, R. V.; Hersh, W. H. Coordination of “Non-coordinating” Anions: Synthesis, Characterization, and X-Ray Crystal Structures of Fluorine-Bridged $[\text{SbF}_6]^-$, $[\text{BF}_4]^-$, and $[\text{PF}_6]^-$ Adducts of $[\text{R}_3\text{P}(\text{CO})_3(\text{NO})\text{W}]^+$. An Unconventional Order of Anion Donor Strength. *Inorg. Chem.* **1989**, *28* (14), 2869–2886.
- (24) Gordon, C. M.; Holbrey, J. D.; Kennedy, A. R.; Seddon, K. R. Ionic Liquid Crystals: Hexafluorophosphate Salts. *J. Mater. Chem.* **1998**, *8* (12), 2627–2636.
- (25) Yuyama, K.; Masuda, G.; Yoshida, H.; Sato, T. Ionic Liquids Containing the Tetrafluoroborate Anion Have the Best Performance and Stability for Electric Double Layer Capacitor Applications. *J. Power Sources* **2006**, *162* (2), 1401–1408.
- (26) Voroshlyova, I. V.; Ferreira, E. S. C.; Malček, M.; Costa, R.; Pereira, C. M.; Cordeiro, M. N. D. S. Influence of the Anion on the Properties of Ionic Liquid Mixtures: A Molecular Dynamics Study. *Phys. Chem. Chem. Phys.* **2018**, *20* (21), 14899–14918.
- (27) Brookhart, M.; Grant, B.; Volpe, A. F. $[(3,5\text{-}(\text{CF}_3)_2\text{C}_6\text{H}_3)_4\text{B}]^-[\text{H}(\text{OEt})_2]^+$: A Convenient Reagent for Generation and Stabilization of Cationic, Highly Electrophilic Organometallic Complexes. *Organometallics* **1992**, *11* (11), 3920–3922.
- (28) Bröring, M.; Kleeberg, C. $[\text{PdCl}(\text{TeMe}_2)_3](\text{BArF})^-$ – The First Structurally Characterized Palladium(II) Complex with TeMe_2 Ligands. *Z. Anorg. Allg. Chem.* **2008**, *634* (5), 946–949.
- (29) Kim, K.-C. Crystallographic Evidence for a Free Silylium Ion. *Science (Washington, DC, U. S.)* **2002**, *297* (5582), 825–827.
- (30) Körbe, S.; Schreiber, P. J.; Michl, J. Chemistry of the Carba-Closo -Dodecaborate(–) Anion, $\text{CB}_{11}\text{H}_{12}^-$. *Chem. Rev.* **2006**, *106* (12), 5208–5249.
- (31) Reed, C. A.; Kim, K. C.; Bolskar, R. D.; Mueller, L. J. Taming Superacids: Stabilization of the Fullerene Cations HC_{60}^+ and C_{60}^+ . *Science (Washington, DC, U. S.)* **2000**, *289* (5476), 101–104.
- (32) Kim, K. C.; Reed, C. A.; Long, G. S.; Sen, A. Et_2Al^+ Alumenium Ion-like Chemistry. Synthesis and Reactivity toward Alkenes and Alkene Oxides. *J. Am. Chem. Soc.* **2002**, *124* (26), 7662–7663.
- (33) Reed, C. A.; Kim, K. C.; Stoyanov, E. S.; Stasko, D.; Tham, F. S.; Mueller, L. J.; Boyd, P. D. W. Isolating Benzenium Ion Salts. *J. Am. Chem. Soc.* **2003**, *125* (7), 1796–1804.
- (34) Knoth, W. H. $1\text{-B}_9\text{H}_9\text{CH}^-$ and $\text{B}_{11}\text{H}_{11}\text{CH}^-$. *J. Am. Chem. Soc.* **1967**, *89* (5), 1274–1275.
- (35) Juhasz, M.; Hoffmann, S.; Stoyanov, E.; Kim, K. C.; Reed, C. A. The Strongest Isolable Acid. *Angew. Chem., Int. Ed.* **2004**, *43* (40), 5352–5355.
- (36) Stoyanov, E. S.; Hoffmann, S. P.; Juhasz, M.; Reed, C. A. The Structure of the Strongest Brønsted Acid: The Carborane Acid $\text{H}(\text{CHB}_{10}\text{Cl}_{10})$. *J. Am. Chem. Soc.* **2006**, *128* (10), 3160–3161.
- (37) Stoyanov, E. S.; Stoyanova, I. V.; Tham, F. S.; Reed, C. A. Evidence for C-H Hydrogen Bonding in Salts of Tert-Butyl Cation. *Angew. Chem., Int. Ed.* **2012**, *51* (36), 9149–9151.
- (38) Nava, M.; Stoyanova, I. V.; Cummings, S.; Stoyanov, E. S.; Reed, C. A. The Strongest Brønsted Acid: Protonation of Alkanes by $\text{H}(\text{CHB}_{10}\text{F}_{10})$ at Room Temperature. *Angew. Chem., Int. Ed.* **2014**, *53* (4), 1131–1134.
- (39) Cummings, S.; Hratchian, H. P.; Reed, C. A. The Strongest Acid: Protonation of Carbon Dioxide. *Angew. Chem., Int. Ed.* **2016**, *55* (4), 1382–1386.
- (40) Saxena, A. K.; Hosmane, N. S. Recent Advances in the Chemistry of Carborane Metal Complexes Incorporating D- and f-Block Elements. *Chem. Rev.* **1993**, *93* (3), 1081–1124.
- (41) Larsen, A. S.; Holbrey, J. D.; Tham, F. S.; Reed, C. A. Designing Ionic Liquids: Imidazolium Melts with Inert Carborane Anions. *J. Am. Chem. Soc.* **2000**, *122* (30), 7264–7272.
- (42) Stoyanov, E. S.; Stoyanova, I. V. Features of Protonation of the Simplest Weakly Basic Molecules, SO_2 , CO , N_2O , CO_2 , and Others by Solid Carborane Superacids. *Angew. Chem.* **2018**, *130* (17), 4606–4610.
- (43) Díaz-Tinoco, M.; Ortiz, J. V. Carborane Superhalide Bases and Their Conjugate Brønsted-Lowry Superacids: Electron Binding Energies and Dyson Orbitals. *Chem. Phys.* **2019**, *521*, 77–84.
- (44) Grabowski, S. J.; Casanova, D.; Formoso, E.; Ugalde, J. M. Tetravalent Oxygen and Sulphur Centres Mediated by Carborane Superacid: Theoretical Analysis. *ChemPhysChem* **2019**, *20* (19), 2443–2450.
- (45) Lipping, L.; Leito, I.; Koppel, I.; Koppel, I. A. Gas-Phase Brønsted Superacidity of Some Derivatives of Monocarba-Closo -Borates: A Computational Study. *J. Phys. Chem. A* **2009**, *113* (46), 12972–12978.
- (46) Lipping, L.; Leito, I.; Koppel, I.; Krossing, I.; Himmel, D.; Koppel, I. A. Superacidity of Closo -Dodecaborate-Based Brønsted Acids: A DFT Study. *J. Phys. Chem. A* **2015**, *119* (4), 735–743.
- (47) Brzeski, J.; Czaplá, M.; Skurski, P. Icosahedral Carborane Superacids and Their Conjugate Bases Comprising H, F, Cl, and CN Substituents: A Theoretical Investigation of Monomeric and Dimeric Cages. *ChemPlusChem* **2020**, *85* (2), 312–318.
- (48) Møller, C.; Plesset, M. S. Note on an Approximation Treatment for Many-Electron Systems. *Phys. Rev.* **1934**, *46* (7), 618–622.
- (49) Head-Gordon, M.; Pople, J. A.; Frisch, M. J. MP2 Energy Evaluation by Direct Methods. *Chem. Phys. Lett.* **1988**, *153* (6), 503–506.
- (50) Frisch, M. J.; Head-Gordon, M.; Pople, J. A. A Direct MP2 Gradient Method. *Chem. Phys. Lett.* **1990**, *166* (3), 275–280.
- (51) Kendall, R. A.; Dunning, T. H.; Harrison, R. J. Electron Affinities of the First-row Atoms Revisited. Systematic Basis Sets and Wave Functions. *J. Chem. Phys.* **1992**, *96* (9), 6796–6806.
- (52) Dunning, J.; Peterson, K. A.; Wilson, A. K. Gaussian Basis Sets for Use in Correlated Molecular Calculations. X. The Atoms Aluminum through Argon Revisited. *J. Chem. Phys.* **2001**, *114* (21), 9244–9253.
- (53) Frisch, M. J.; Trucks, G. W.; Schlegel, H. B.; Scuseria, G. E.; Robb, M. A.; Cheeseman, J. R.; Scalmani, G.; Barone, V.; Petersson, G. A.; Nakatsuji, H.; et al. *Gaussian 16*, Rev. B.01; Gaussian Inc.: Wallingford, CT, 2016.
- (54) Christie, K. O.; Dixon, D. A.; McLemore, D.; Wilson, W. W.; Sheehy, J. A.; Boatz, J. A. On a Quantitative Scale for Lewis Acidity and Recent Progress in Polynitrogen Chemistry. *J. Fluorine Chem.* **2000**, *101* (2), 151–153.
- (55) Valadbeigi, Y.; Gal, J.-F. Organometallic Superacids and Hyperacids: Acidity Enhancement by Internal Bonding with a Strong Electron-Pair Acceptor Group BX_2 . *Chem. Phys. Lett.* **2021**, *763*, 138207.
- (56) Valadbeigi, Y.; Kurtén, T. Clustering of H_2SO_4 with BX_3 ($X = \text{H}, \text{F}, \text{Cl}, \text{Br}, \text{CN}, \text{OH}$) Compounds Creates Strong Acids and Superacids. *Comput. Theor. Chem.* **2019**, *1153*, 34.